Title

DETERMINATION OF ROCK FRACTURE PARAMETERS FROM CRACK MODELS FOR FAILURE IN COMPRESSION

Authors

Kemeny, J.M.
Cook, N.G.W.

Publication Date

1987-05-01

Lawrence Berkeley Laboratory
UNIVERSITY OF CALIFORNIA

EARTH SCIENCES DIVISION

Presented at the 28th U.S. Symposium on Rock Mechanics, Tucson, AZ, June 29–July 1, 1987, and published in the Proceedings

Determination of Rock Fracture Parameters from Crack Models for Failure in Compression

J.M. Kemeny and N.G.W. Cook

May 1987

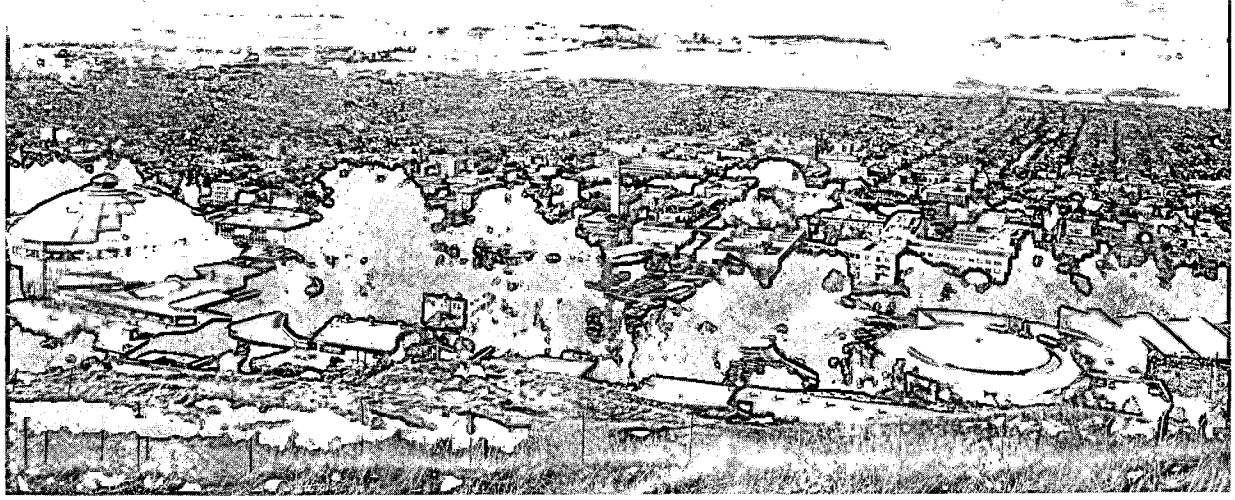

Prepared for the U.S. Department of Energy under Contract Number DE-AC03-76SF00098.

DISCLAIMER

REFERENCES

Aki, K. 1979. Characterization of barriers on an earthquake fault. J. Geophys. Res. 84:6140-6148.

Ashby, M. F., and Hallam, S. D. 1986. The failure of brittle solids containing small cracks under compressive stress states. Acta Metall. 34:497-510.

Brace, W. F. , Paulding, B. W. , and Sholtz, C. 1966. Dilatancy in the fracture of crystalline rocks. J. Geophys. Res. 77:3939.

Costin, L. S. 1985. Damage mechanics in the post failure regime. Mech.of Mat. 4:149-160.

Detournay, E., and Roegiers, J.-C. 1986. Comment on 'Well bore breakouts and in situ stress', by Zoback, Moos, Mastin, and Anderson. J. Geophys. Res. 91:14161-14162.

Evans, B. and Wong, T.- f. 1985. Shear localization in rocks induces by tectonic deformation. In Mechanics of Geomaterials, edited by Z. Bazant, John Wiley and Sons.

Ewy, R. T., Kemeny, J. M., Zheng, Z., and Cook, N. G. W. 1987. Generation and analysis of stable excavation shapes under high rock stresses. To appear, Sixth Int. Cong. on Rock Mech., Montreal, Canada.

Fairhurst, C. and Cook, N. G. W. 1966. The phenomenon of rock splitting parallel to a free surface under compressive stress. Proc. First Cong. Int. Soc. Rock Mech, Lisbon. 1:687-692.

Fredrich, J. T., and Wong, T.-f. 1986. Micromechanics of thermally induced cracking in three crustal rocks. J. Geophys. Res. 91:12743-12764.

Hadley, K. 1976. Comparison of calculated and observed crack densities and seismic velocities in Westerly granite. J. Geophys. Res. 81:3484.

Hallbauer, D.K., Wagner, H., and Cook, N.G.W. 1973. Some observations concerning the microscopic and mechanical behavior of quartzite specimens in stiff, triaxial compression tests. Int. J. Rock Mech. Min. Sci. 10:713-726.

Horii, H. and Nemat-Nasser, S. 1985. Compression induced microcrack growth in brittle solids: axial splitting and shear failure. J. Geophs. Res. 90: 3105-3125.

Jaeger, J. C. and Cook, N.G.W. 1976. Fundamentals of Rock Mechanics. Halsted Press, N.Y.

Kemeny, J. M., and Cook, N. G. W. 1987. Crack models for the failure of rock under compression. Proc. 2nd Int. Conf. Constitutive Laws for Eng. Mat. 2:879-887.

Kranz, R. L. 1983. Microcracks in rocks: a review. Tectonophysics. 100:449-480.

Rice, J. R. 1980. The mechanics of earthquake rupture. In Physics of the Earth's Interior, edited by A. M. Dziewonski and E. Boschi, Italian Physical Society, Bologna, Italy .

Rudnicki, J. W. 1980. Fracture mechanics applied to the earth's crust. Annu. Rev. Earth Planet. 8:489-525.

Sammis, C. G., and Ashby, M. F. 1986. The failure of brittle porous solids under compressive stress states. Acta Metall. 34:511-526.

Scholz, C. H., Boitnott, G, and Nemat-Nasser, S. 1986. The bridgeman ring paradox revisited. PAGEOPH. 124:587-599.

Sibson, R. H. 1986. Brecciation processes in fault zones: inferences from earthquake rupturing. PAGEOPH. 124:159-175.

Tapponier, P., and Brace, W. F. 1976. Development of stress induced microcracks in Westerly granite. Int. J. Rock Mech. Min. Sci. 13:103.

Wawersik, W.R., and Fairhurst, C. 1970. A study of brittle rock fracture in laboratory compression experiments. Int. J. Rock Mech. Min. Sci. 7:561-575 .

Wawersik, W. R. and Brace, W. F. 1971. Post-failure behavior of a granite and diabase. Rock Mech. 3:61-85.

Wong, T.- f. 1982. Shear fracture energy of Westerly granite from post-failure behavior. J. Geophys. Res. 87:990-1000.

Wong, T.- f. 1985. Geometric probability approach to the characterization and analysis o f microcracking in rocks. Mechanics of Materials. 4:261-276.

macroscopic fracture. Thus for the splitting of Westerly granite under uniaxial or low values of confining stress as measured by Wawersik and Brace (1971), we assume that a single splitting crack or at most a few such fractures result. In this way, all the energy involved in subsidiary crack growth around the main splitting or shear fractures is taken into account. Using equation (5) and the G_{tot} values for splitting as given is section 2, the G_c value for a single splitting crack becomes 0.93×10^4 J/m^2. Comparing this value with the value of G_c for a microcrack as given in section 2 by 16.4 J/m^2, we see that there is a difference of three orders of magnitude. This indicates that the formation of splitting cracks under compressive stresses involves the creation of a large amount of subsidiary crack surface area, which absorbs strain energy and causes an apparent G_c that is much larger than the actual G_c at the tip of the crack. The excess crack surface area is created because the initial axial crack growth is a stable process as reflected in the strain hardening stress stain curves for the splitting model, allowing cracks of different sizes to extend. This can be compared with the formation of fractures under direct tensile stresses. This is an unstable process, resulting in a macrocrack with very little subsidiary microcracking, and results in G_c values of 1-100 J/m^2, which is in the range of the values calculated for the microcracks, as discussed in section 2. Also, it can be expected that for the formation of large joints on the order of tens of meters, another level of scale effects will occur that will cause the G_c values to be even larger.

For the shear faulting model, we calculate a G_c value for the creation of a single shear fault of 1.05 J/m^2. There is very little difference between this value of G_c and the G_c value estimated for the shear faulting model in section 2, since in both cases we only consider the formation of a single shear plane, without subsidiary microcracking. As discussed in section 2, the shear faulting model applies in the region past the peak stress after the shear fault has been formed, and does not include the initial growth of tensile cracks. Thus the shear faulting model applies to the situation where a throughgoing shear fault already exists. Also, it is assumed that the fault plane is planar. Work by Sibson (1986) and others have shown that faults often consist of en echelon segments, and the shear of such an en echelon pattern of fault segments can create local regions under compressive, tensile, and shear stresses. Thus complex patterns of subfaulting around a main fault can occur, and this subfaulting can result in a large increase in the large scale G_c, as shown for the case of splitting cracks.

4 CONCLUSIONS

We have used the splitting and shear fracture models of Kemeny and Cook (1987) to look at fracture parameters associated with different scales of fracturing. At the smallest scale, we consider microcracks with lengths and spacings on the order of the mineral grains, and on a larger scale, we consider the growth and coalescence of these microcracks into splitting fractures or shear faults on the order of the size of the laboratory samples. From these two scales we can further extrapolate to the scales of joints and faults in the field. The primary fracture parameter that we study is the fracture energy, G_c. We find that the G_c associated with microcracking is at least three orders of magnitude less than the G_c associated with the propagation of the sample size fractures. This is due to the fact that the propagation of large scale fractures under compressive stresses is associated with the creation of crack surface area not only in the large scale fracture itself but also in the neighborhood of the fracture. This applies both to the creation of splitting fractures and shear faults. Thus G_c is a very scale dependent parameter that depends strongly on the details of the substructure of large fractures. This gives an explanation for the wide range of values of G_c from 10^2 to 10^8 J/m^2 that are reported in the literature (Wong, 1982).

ACKNOWLEDGEMENTS

This work was supported by the Director, Office of Basic Energy Sciences, Division of Engineering, Mathematics, and Geosciences, of the U. S. Department of Energy under contract DE-AC03-76SF00098.

propagate in plane, when $G = G_c$. A closed from solution for the shear model is given by the two equations below:

$$\varepsilon_1 = \frac{4\tau^* b \cos\beta (1-\nu^2)}{\pi w E} \ln \cos(\pi l/2b) + \frac{\sigma_1}{E'} \qquad (8)$$

$$\sqrt{(G_c E')} = \tau^* [2b \tan(\pi l/2b)]^{1/2} \qquad (9)$$

where τ^* is given in equation (4). A G_c value to go into the shear model in equation (9) was determined using the same method as outlined for the splitting model. The shear faulting model takes into account the shear localization processes but does not take into accound the initial axial growth of cracks. Thus G_{tot} for the shear faulting model was calculated only in the region of the stress strain curve past the peak stress, at which point it is assumed that a throughgoing shear fault has been formed (Hallbauer et al., 1973, Wong, 1982). Also, because data from triaxial tests are used in the shear faulting model, there will be an additional contribution to the crack energy in equation (7) due to lateral expansion against the applied confining pressure (Wong, 1982). However, because the shear faulting model as given in equations (8) and (9) gives no volume expansion, equation (7) can still be used, the only modification being that the uniaxial stress σ_1 in equation (7) is replaced by the effective axial stress $\sigma_1 - \sigma_3$. The 1500 psi curve from Wawersik and Brace (1971) was used in the calculation of G_c, giving a G_c value of 1.40 x 10^4 J/m^2. Results of the shear faulting model are shown in Figure 2b. As before, the curves in Figure 2b show initial linear behavior prior to the extension of the shear cracks. Now, however, extension of the shear cracks results in only strain softening behavior. Also, the strain softening slopes show regions of both class I and class II behavior, as opposed to the splitting model, where the behavior past the peak stress was predominantly Class II. Also, the increase in strength for the shear model with increasing confining pressure is much less pronounced than it was with the splitting model. This is in agreement with the data from Wawersik and Brace (1971).

Even though two separate models were used, the splitting and shear models discussed above correctly predict the transition from splitting to shear faulting as the confining stress is increased. At low values of confining stress, splitting behavior is predicted, since the peak stresses are lower for the splitting model at these values of confining stress. However, as the confining stress is increased, the peak stresses for the splitting model increase much more rapidly than for the shear model, and thus the models predict that at confining stresses of around 1500 psi, the shear model has lower peak strengths and is thus the favored mode of failure.

3 LARGE SCALE FRACTURE ENERGIES

Even though the formation of macroscopic splitting or shear fractures is a complicated process involving the growth, interaction, and coalescence of microcracks, it is often of interest to model this phenomena on a larger scale as the growth of a single fracture. This would occur, for instance, in analysing the formation of joints sets under regional compressive stresses, the spalling of underground openings, and the occurrence of earthquake rupture. Thus we want to determine from laboratory triaxial tests properties that are relevant on a larger scale. These large scale properties must take into account the extent of crack surface area that is created on the microscopic level. We have shown in section 2 how the properties of the microcracks can be determined from laboratory tests. Here we show how macroscopic properties are determined from laboratory triaxial results. By comparing these results with the results for microcracks, we gain some qualitative information into scale effects.

The method of calculating G_c for the macroscopic splitting and shear faults is essentially the same as the calculation of microscopic properties from laboratory test results, except now, the total crack energy, G_{tot}, is divided by the surface area of a single

energy is due to crack growth. ε_i is the inelastic axial strain, and is calculated at a given stress level by subtracting out the elastic axial strain, i.e., $\varepsilon_i = \varepsilon_1 - \sigma_1/E$. The integral is from $\varepsilon_i = 0$ to $\varepsilon_i = \varepsilon_{max}$, where ε_{max} is the maximum value of strain. For rocks exhibiting class II softening, ε_i may reach a maximum and then decrease to a final value, ε_{fin}. For this case the single integral in equation (7) is replaced by two integrals, the first integral from 0 to ε_{max}, and the second integral from ε_{max} to ε_{fin}. Also, we have taken out of the integral the energy due to friction along the initial crack surfaces, since this energy does not contribute to the deformation of the sample. σ_f is the frictional stress under a given value of axial stress, and assuming that all the initial cracks have an average angle θ, then $\sigma_f = \mu\sigma_1\cos^2\theta$.

For the uniaxial test by Wawersik and Brace (1971), this method gives a G_{tot} of approximately 12.1 Joules. $N(l_f - l_o)T$ was estimated from data given in Wawersik and Brace (1971) and Wong (1985) to be approximately 0.74 m^2. Thus we get a G_c value for axial microcrack growth from the uniaxial test of Wawersik and Brace (1971) of approximately 16.4 J/m^2. Assuming that all of this energy went into tensile crack extension, K_{IC} is determined using the relationship $K_{IC} = \sqrt{(G_c E')}$, which gives a K_{IC} value of approximately 0.99 MPa$\sqrt{m}$, which is in the range of K_{IC} values measured in standard K_{IC} tests (0.5 - 2.0 MPa$\sqrt{m}$).

Another parameter that is needed for the splitting model is the initial crack density, given by Nl_o^2/V. Based on data in Wong (1985), we have used an initial crack density of 0.25. E and ν are taken to be 6×10^{10} Pa and 0.2, respectively. Also, it is assumed that on average the initial cracks have a coefficient of friction $\mu = 0.4$ and an initial angle of 45 degrees, and thus sliding on the initial cracks and the extension of the wing cracks will occur on all the cracks simultaneously.

The results of the splitting model at three values of confining stress, using the above parameters, are presented in Figure 1b. The curves in Figure 1b show initial linear behavior due to sliding on the initial cracks of length l_o, before the tensile wing cracks begin to grow. Strain hardening is exhibited as the wing cracks grow initially, and as the wing cracks interact with each other, class II softening is exhibited. Both the magnitudes of the stresses and strains, and the general shape of the stress strain curves, match very well with the uniaxial and low confinement data of Wawersik and Brace (1971). In particular the occurrence of class II softening in the splitting model, and the large increases in the peak stress with small increases in confinement match with the experimental data of Wawersik and Brace (1971). For larger increases in confining stress, shear faulting is the dominant mechanism, and the splitting model predicts too large increases in peak stress with increasing confining stress.

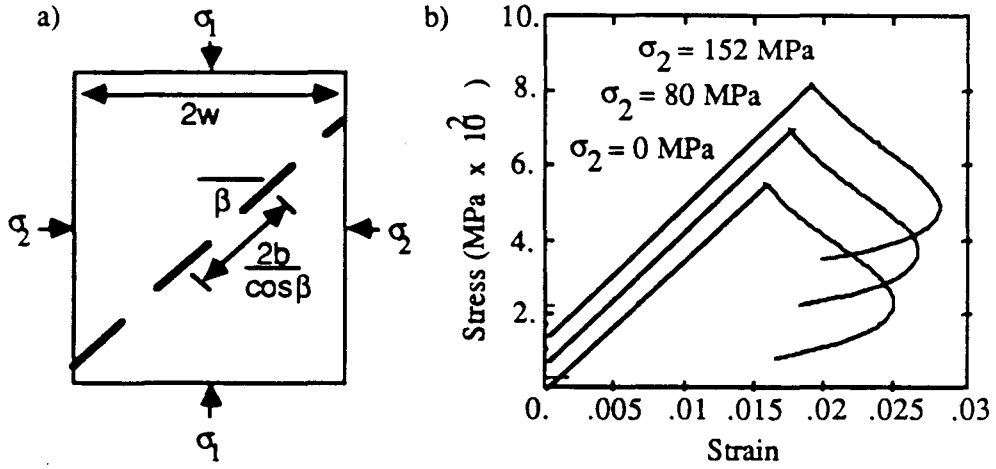

Figure 2. Shear faulting model

The shear faulting model of Kemeny and Cook (1987) is shown in Figure 2a, and consists of a collinear row of cracks at an angle β, and it is assumed that the cracks

Here we review some of the results of the splitting and shear failure models of Kemeny and Cook (1987). The axial splitting model of Kemeny and Cook (1987) is shown in Figure 1a, and consists of a two dimensional (plane strain) body of height 2h and width 2w containing a column of sliding cracks of initial length l_o, angle θ, and separation 2b. Also, the surface of the initial cracks have a constant coefficient of friction μ. For this model a closed form analytic solution has been derived as given by the two equations below:

$$\varepsilon_1 = \frac{4\sin\theta\, l_0 (1-\nu^2)}{\pi E w b}\left[\frac{\tau^* \pi^2 l_0}{8\cos\theta} + \tau^* l_0 \cos\theta \ln\frac{\tan(\pi l/2b)}{\tan(\pi l_0/2b)} - \sigma_2 b \ln\frac{\tan(\pi/4(1+l/b))}{\tan(\pi/4(1+l_0/b))}\right] \quad (3)$$

$$K_{IC} = \frac{2 l_0 \tau^* \cos\theta}{\sqrt{(b\sin(\pi l/b))}} - \sigma_2 \sqrt{(2b\tan(\pi l/b))} \quad (4)$$

where $\tau^* = 1/2\,[(\sigma_1 - \sigma_2)\sin 2\theta - \mu(\sigma_1 + \sigma_2 + (\sigma_1 - \sigma_2)\cos 2\theta)]$

Equation (3) describes the effective linear stress strain behavior due to sliding cracks with a given wing crack length and spacing between sliding cracks, and equation (4) gives the value of axial stress at which cracking starts for that geometry, based on crack growth criterion $K_I = K_{IC}$. Together, the two equations describe the nonlinear constitutive behavior due to progressive crack growth (two equations are the minimum in order to describe non-functional behavior such as class II softening). Using uniaxial data by Wawersik and Brace (1971) and crack statistics data from Wong (1985), we have estimated the K_{IC} value to go into equation (4) as follows. First of all, we assume G_c is constant, and using the definition of G as given in section 1.0, we get the following relationship:

$$G_{tot} = G_c * S_{tot} \quad (5)$$

where G_{tot} represents the total energy absorbed by the creation of new crack surface area in a uniaxial test, and S_{tot} represents the total change in crack surface area due to the uniaxial test. We determine G_{tot} from complete stress strain curves from laboratory tests, and we determine S_{tot} from crack statistics data. The crack statistics are usually made on two dimensional slices through laboratory samples, and therefore we assume the cracks are two dimensional and revise equation (5) as follows:

$$G_{tot} = G_c * N(l_f - l_o)T \quad (6)$$

where l_f is the average final crack length, l_o is the average initial crack length, N is the number of cracks as measured in a two dimensional section, and T is the effective thickness of the sample. These are parameters that can be estimated from crack statistics data, as determined for Westerly granite by Wawersik and Brace (1971), Hadley (1976), Tapponier and Brace (1976), Fredrich and Wong (1984), Wong (1985), and others. G_{tot} is determined by estimating the following integral from uniaxial laboratory data:

$$\frac{G_{tot}}{V} = \int_0^{\varepsilon_{max}} (\sigma_1 - \sigma_f)\, d\varepsilon_i \quad (7)$$

where V is the volume of the sample. This integral represents the energy per unit volume due to inelastic processes, and it is assumed in this paper that all this inelastic

growth occurs when:

$$G = G_c \tag{1}$$

G depends on the loading and crack geometries, while G_c is a material property based on the micromechanical breakdown processes at the crack tip (Rice, 1980). Also, G is related to the crack tip stress intensity factors by:

$$G = \frac{K_I^2}{E'} + \frac{K_{II}^2}{E'} + \frac{K_{III}^2}{E}(1 + \nu) \tag{2}$$

where K_I, K_{II}, and K_{III} are the modes I, II, and III stress intensity factors, $E' = E$ for plane stress and $E' = E/(1 - \nu^2)$ for plane strain, where E is the Young's modulus and ν is Poisson's ratio. Under pure mode I loading, equations (1) and (2) reduce to $G_c = K_I^2/E'$ (equivalent to the relation $K_I = K_{IC}$, where K_{IC} is referred to as the fracture toughness). Under pure mode II loading, equations (1) and (2) give the relation $G_c = K_{II}^2/E'$.

Rice (1980) presented a method for determining G_c for shear faulting (mode II) by integrating the area under the stress strain curve in laboratory triaxial tests, and Wong(1982) used this method to determine G_c values for Westerly granite, getting values of around 10^4 Joules/m^2. Values of G_c for earthquake faulting have also been determined from seismic data (Aki, 1979; Rudnicki, 1980), in the range of 10^3 - 10^8 J/m^2. The large difference between laboratory and field determined values of G_c for shear faulting indicates that scale effects exist. Also, measurements of G_c in standard fracture toughness tests for mode I cracking give values of G_c between 1 - 10 J/m^2. In this paper, we determine G_c values for both splitting and shear faulting using triaxial test data. The fracture energy associated with splitting is important for the behavior of rock adjacent to underground openings, joint formation, and borehole breakout (Ewy et al, 1987), while the fracture energy associated with shear faulting is important for the genesis of faults, and the process of earthquake rupture (Rice, 1980). Our calculations of G_c are based on the complete stress strain curves for Westerly granite determined by Wawersik and Brace (1971). In particular, for uniaxial and low values of confining stress, splitting fractures are formed, and the G_c values represent the energy to form splitting fractures. At higher values of confining stress, shear faults are formed, and the G_c values represent the energy to create shear faults. In addition to calculating the fracture energies associated with splitting and faulting, we also use the triaxial data of Wawersik and Brace (1971), along with crack statistical data of Wong (1985), to determine G_c values associated with the growth of microcracks that interact and coalesce to form macroscopic splitting and shear faults. We find that the G_c values associated with macroscopic splitting and faulting can be several orders of magnitude greater than the energies associated with the growth of microcracks, and this difference can explain the scale effects that have been reported (Wong, 1982).

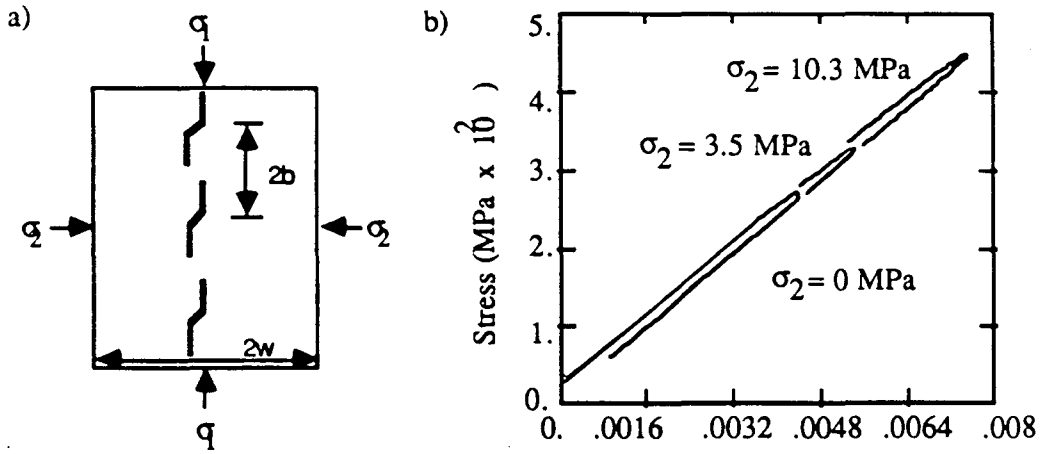

Figure 1. Axial splitting model

failure regime, rocks exhibit strain softening behavior. Strain softening can be unstable, depending on the imposed boundary conditions and the slope of the stress strain curve in the strain softening region (Jaeger and Cook, 1979). The potential instability of strain softening slopes make them difficult to measure, however it is for exactly this reason that it is important to understand the mechanisms responsible for this behavior. Wawersik and Fairhurst (1970) and Wawersik and Brace (1971), measured complete stress strain curves on a variety of rocks in uniaxial and triaxial compression, and they classified complete stress-strain curves into two categories, based on the characteristics of the post failure behavior. Class I refers to rocks that exhibit 'normal' strain softening behavior past the peak stress, i.e., where the decrease in stress past the peak stress is accompanied by an increase in strain (negative slope). These strain softening slopes are unstable under stress controlled boundary conditions, but stable under displacement controlled boundary conditions. Class II refers to rocks in which the stress strain curves loop back towards the origin, in other words, the decrease in stress past the peak stress is accompanied by a decrease in strain (positive slope). These strain softening slopes are unstable under all boundary conditions.

In order to understand the above phenomena, micromechanical models for the failure of rock in compression have been developed. These include models for splitting at low values of confining stress, and for shear faulting at higher values of confining stress. Many of the models for axial splitting are based on the 'sliding crack', as developed originally by Brace et al.(1966) and Fairhurst and Cook (1966). The sliding crack consists of an initial, planar microcrack under shear and normal stresses derived from the externally applied triaxial stresses. Once the frictional forces along this initial crack have been exceeded, the crack faces will slide past one another, forming tensile stresses in the regions near the crack tips. Under continued loading, the tensile stresses will increase until two tensile 'wing cracks' emerge symmetrically from both ends of the initial crack, and as the wing cracks propagate they orient themselves in the direction of the maximum principle stress. Fracture models for axial splitting based on the sliding crack include Horii and Nemat-Nasser (1985), Ashby and Hallam (1986), and Kemeny and Cook (1987). These models consider single or multiple sliding cracks in a linear elastic matrix, and nonlinear stress strain relationships are derived that exhibit strain hardening and strain softening due to the propagation and interaction of the tensile wing cracks. The sliding crack has also been used to explain the mechanics of borehole breakout (Detournay and Roegiers, 1986) and discing in compressed rock cores (Scholz et al., 1986). Models for axial splitting under triaxial compression that do not use the sliding crack include Costin, 1985 (tensile crack growth due to prescribed regions of tension), and Sammis and Ashby, 1986 (tensile crack growth due to stress concentrations around circular openings).

With regards to shear faulting, micromechanical models have been developed by Nemat-Nasser and Horii (1985) and Kemeny and Cook (1987). Nemat-Nasser and Horii (1985) model shear faulting by lining up sliding cracks at some angle to the maximum principle stress, and finding conditions for the sliding cracks to become unstable due to crack interaction. This model does not take into account some of the shear processes that operate during shear localization, such as microbuckling of columns of rock formed by the initial axial growth of microcracks, kinking within mineral grains, and rotation and crushing of microblocks (Wong and Evans, 1985). Kemeny and Cook (1987) consider a collinear row of cracks at an angle to the maximum principle stress, and allow the cracks to grow in the plane of the cracks assuming a shear fracture energy criterion. This model is a simplification of the processes in shear localization, and does not include the initial tensile crack growth that occurs prior to shear localization. Thus this model is expected to apply in the region of the stress strain curve after stabilization of the initial axial cracks has occurred.

In this paper, the micromechanical models of Kemeny and Cook (1987) for splitting and shear faulting are used to investigate parameters associated with rock fracture under compressive stresses. Fracture properties exist both on the scale of microcracks, and on the scale of the macrofractures formed by the coalescence of microcracks. One of the most important parameters with regards to fracture is the critical energy release rate, G_c. G is defined as the amount of energy release per unit increase in crack surface area, and crack

28th US Symposium on Rock Mechanics / Tucson / 29 June-1 July 1987

Determination of rock fracture parameters from crack models for failure in compression

John M.Kemeny
Lawrence Berkeley Laboratory, Berkeley, Calif., USA
Neville G.W.Cook
University of California, Berkeley, USA

ABSTRACT

Micromechanical models for axial splitting and for shear faulting are used to investigate parameters associated with rock fracture under compressive stresses. The fracture energies to create splitting fractures and shear faults are calculated using laboratory triaxial data. These energies are compared with the fracture energies for the propagation of microcracks that coalesce to form the larger scale fractures. It is found that for Westerly granite, the energies to create splitting fractures and shear faults are about three orders of magnitude greater than the energy needed to drive the tensile microcracks, due to the large amount of subsidiary crack surface area created in forming the larger scale fractures. A similar scale effect can be expected when extrapolating the laboratory results to field scale problems.

1 INTRODUCTION

Much of the research in rock mechanics has been concerned with the failure of small, laboratory specimens of rock under compressive stresses. It is supposed that such failure is analogous to large scale problems such as the failure and stability of wall rock in underground openings, the formation of joints, and the propagation of faults in earthquake rupture. Even though a large data base of information has been gathered on rock failure in compression for many different rock types and under a variety of conditions, the mechanisms responsible for this behavior are still not fully understood. Stress strain relations associated with the failure of brittle rocks under compressive stresses are highly nonlinear and path dependent, due primarily to the complex nature of the microstructure on the scale of mineral grains, and to anisotropic changes in the microstructure during compressive loading. For instance, a brittle rock such as granite contains mineral constituents with differing material properties, and defects such as microcracks and pores. Hallbauer et al. (1973), Kranz (1983), Wong (1985) and others show that before load is applied to a laboratory sample, the microcracks in brittle rocks have a relatively homogeneous distribution and often random orientations related to the genesis of the rock. As rock samples are loaded in compression, the crack density increases, along with an anisotropy in crack orientation due to crack growth in the direction of the maximum principle stress. With further loading, these axially growing cracks interact and coalesce to form macroscopic features such as splitting fractures under uniaxial compression or shear faults under triaxial compression (Horii and Nemat-Nasser, 1985). These macroscopic features are important in understanding the evolution of natural joints and faults in rock, and in determining parameters associated with spalling around underground openings, joint formation, and earthquake rupture (Wong, 1982).

In general, rocks tested under compression exhibit linear elastic or strain hardening stress-strain behavior up to a peak stress. Past the peak stress, referred to as the post

LAWRENCE BERKELEY LABORATORY
TECHNICAL INFORMATION DEPARTMENT
UNIVERSITY OF CALIFORNIA
BERKELEY, CALIFORNIA 94720